

Polymorph-Dependent Solid-State Fluorescence and Selective Metal-Ion-Sensor Properties of 2-(2-Hydroxyphenyl)-4(3*H*)-quinazolinone

Savarimuthu Philip Anthony^{*[a]}

Abstract: 2-(2-Hydroxy-phenyl)-4(3*H*)-quinazolinone (HPQ), an organic fluorescent material that exhibits fluorescence by the excited-state intramolecular proton-transfer (ESIPT) mechanism, forms two different polymorphs in tetrahydrofuran. The conformational twist between the phenyl and quinazolinone rings of HPQ leads to different molecular packing in the solid state, giving structures that show solid-state

fluorescence at 497 and 511 nm. HPQ also shows intense fluorescence in dimethyl formamide (DMF) solution and selectively detects Zn^{2+} and Cd^{2+} ions at micromolar concentrations in DMF. Importantly, HPQ not only detects

Keywords: fluorescence • organic solid-state fluorescence • polymorphism • sensors

Zn^{2+} and Cd^{2+} ions selectively, but it also distinguishes between the metal ions with a fluorescence λ_{max} that is blue-shifted from 497 to 420 and 426 nm for Zn^{2+} and Cd^{2+} ions, respectively. Hence, tunable solid-state fluorescence and selective metal-ion-sensor properties were demonstrated in a single organic material.

Introduction

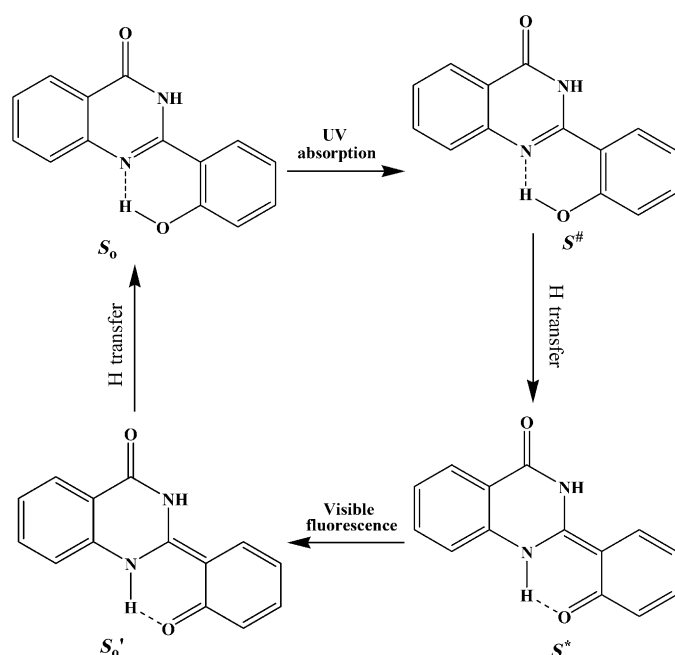
Organic fluorescent molecules have long been attracting scientists' interest owing to their applications in electronics, optics, and sensors.^[1] In particular, developing molecules with strong fluorescence in both the solid state as well as in solution with structural features that enable guest interaction would be interesting, because that might allow both optoelectronic and sensor applications to be realized in a single material. The emergence of photonic and optoelectronic technology such as organic light-emitting diodes (OLEDs), solid lasers, and fluorescence sensors in recent years have spurred demand for strong solid-state-fluorescent molecules.^[2] However, synthesizing highly efficient solid-state-fluorescent organic molecules is a challenging task, because the molecular aggregation of chromophores, which is inherent in the solid state, typically results in the concentration quenching of fluorescence.^[3] Furthermore, obtaining different crystalline phases (polymorphs) in such fluorescent molecule provides the best opportunity to investigate the relationship of molecular packing with optical properties as well as to obtain tunable solid-state-fluorescent materials without doing further synthesis.^[4–6] Solid-state fluorescence of molecular materials has also been tuned either by modification of substitutions on a single molecule^[7] or by supramolecular chemistry.^[8]

Similarly, finding fluorescent organic molecular probes that selectively bind metal ions, particularly Zn^{2+} and Cd^{2+} ions, has also currently been of interest due to the biological role of these ions.^[9] Such molecular sensors are important, because although both metal ions often induce similar spectral changes while coordinated to fluorescent sensors, they play totally different roles in biochemical processes. Zn^{2+} is the second-most-abundant transition-metal ion in the human body and is involved in many important biological activities.^[10] On the contrary, Cd^{2+} is known as a toxic metal ion and can cause serious diseases, such as renal dysfunction, calcium metabolism disorders, prostate cancer, and so forth.^[11] However, fluorescent sensors that distinguish between Zn^{2+} and Cd^{2+} metal ions are rarely reported.^[12]

2-(2-Hydroxy-phenyl)-4(3*H*)-quinazolinone (HPQ), a typical organic compound that exhibits solid-state fluorescence by excited-state intramolecular proton-transfer (ESIPT) reaction (Scheme 1), has been reported to show good photophysical properties, such as intense fluorescence, and can be used as a fluorescent ink and precipitating substrate for various enzymes.^[13] However, crystal-structure investigation has never been explored in HPQ. The presence of the hydroxy pyridyl metal chelating group and intense solid-state fluorescence indicates HPQ might be an interesting material to explore polymorphism and metal-ion-sensor properties. HPQ derivatives are scarcely used as chemical sensors in analytical chemistry.^[14] Structurally similar 2-(2'-hydroxyphenyl)imidazo[1,2-*a*]pyridine, which exhibits solid-state fluorescence by ESIPT shows polymorphism and tunable fluorescence.^[6] Hence, we expected that HPQ also might form polymorphic structures in suitable solvent conditions. Herein, we demonstrate concomitant polymorph formation of HPQ from THF solvent and polymorph-dependent solid-state fluorescence. HPQ forms polymorphic structures

[a] S. P. Anthony
School of Chemical & Biotechnology, SASTRA University
Thanjavur-613 403, Tamil Nadu (India)
Fax: (+91) 4362264120
E-mail: philip@biotech.sastra.edu

Supporting information for this article is available on the WWW under <http://dx.doi.org/10.1002/asia.201100832>.



Scheme 1. Basic mechanism for ESIPT reaction of HPQ.

owing to the difference in the conformational twist between the phenyl and quinazolinone rings. Interestingly, HPQ that exhibits strong fluorescence in dimethyl formamide (DMF; $\Phi=0.21$) selectively detects and differentiates Zn^{2+} and Cd^{2+} metal ions at micromolar concentrations. Thus, both the tunable solid-state fluorescence and sensor phenomena have been demonstrated in a single fluorescent organic material, HPQ.

Results and Discussion

HPQ, a quinazolinone derivative, was obtained by an unprecedented yet simple synthetic method. The intended hydrolysis of 2-(2'-cyanophenoxy)benzonitrile (O,O-CN) in ethanol/water mixture (80:20) in the presence of NaOH to obtain the corresponding acid, 2,2'-oxybis(benzoic acid), lead to the formation of HPQ (98%) exclusively as a single product. Surprisingly, the expected corresponding carboxylic acid did not form at all. Use of methanol instead of ethanol also gives HPQ exclusively. However, hydrolysis of O,O-CN in water alone with NaOH produces the corresponding acid, 2,2'-oxybis(benzoic acid) in 85% yield and only 10% HPQ. The reaction mechanism and the role of alcohol were not clear at this stage. Several synthetic approaches have been reported for the synthesis of HPQ.^[15]

HPQ powder obtained from the reaction solution shows blue solid-state fluorescence. Recrystallization of HPQ from ethyl acetate, ethanol, methanol, acetone, DMF, DMSO, and chloroform gave crystals with plate morphology that exhibit blue solid-state fluorescence ($\lambda_{\text{max}}=497$ nm, excitation wavelength 370 nm). However, crystallization of HPQ from THF produced crystals with needle as well as plate mor-

phology. Excitation of needle-morphology crystals at 370 nm gives blue-green fluorescence, and plate-morphology crystals show blue fluorescence (Figure 1). Blue and blue-green

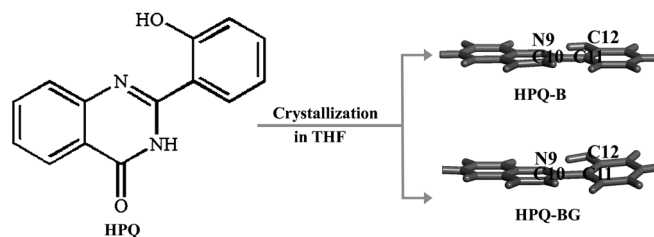


Figure 1. Schematic diagram of HPQ solid state fluorescence tuning via polymorphism.

emitting crystals are hereafter referred to as HPQ-B and HPQ-BG, respectively. Single-crystal X-ray analysis was performed to get an insight into the HPQ molecular assembly in the solid state. Single-crystal analysis revealed different structural arrangements of HPQ molecules in the crystal lattices of HPQ-B and HPQ-BG (Figure 2). Both HPQ-B and HPQ-BG formed strong amide...amide intermolecular and OH...N intramolecular H-bonding interactions in the crystal lattice.^[16] The amide...amide intermolecular interactions lead to the formation of HPQ dimers in both crystal lattices (Figure 2c,d). However, both the amide...amide intermolecular and OH...N intramolecular H-bonding distances of HPQ-BG are slightly shorter than in the HPQ-B polymorph.

HPQ dimers of HPQ-B and HPQ-BG are further interconnected through $\pi\cdots\pi$ interactions in the crystal lattices (Figure 3). In addition, polymorph HPQ-BG shows O...H-C intermolecular interaction between hydroxy oxygen atoms and quinazolinone aromatic hydrogen atoms and carbonyl...carbonyl dipolar ($\text{C}=\text{O}^{\delta-}\cdots\text{C}^{\delta+}=\text{O}$) interactions in the crystal lattice (Figure 3b).^[17] The O...H-C intermolecular interactions of HPQ-BG lead to the formation of two-dimensional sheets in the crystal lattice (Figure 3c). The most notable structural difference of the HPQ molecule in the two crystal lattices is the conformational difference of the N9-C10-C11-C12 dihedral angle θ between the phenyl and quinazolinone rings (Figure 1). While the two aromatic rings are less twisted ($\theta=3.68^\circ$) in polymorph HPQ-B, they are more twisted in HPQ-BG ($\theta=9.97^\circ$). The conformational differences of phenyl and quinazolinone rings lead to different molecular packing in the solid state (Figure 2). The formation of slightly stronger H-bond interactions, additional O...H-C, and $\text{C}=\text{O}^{\delta-}\cdots\text{C}^{\delta+}=\text{O}$ dipolar intermolecular interactions might be the stabilizing force in the more twisted conformation of HPQ in HPQ-BG.

The crystalline solids of HPQ-B and HPQ-BG were ground to powders and examined by powder X-ray diffraction. In each case, the observed PXRD pattern closely matched the theoretical PXRD pattern calculated from the corresponding single-crystal structure, thus indicating that these bulk powders had the same overall structure as their crystalline solids (Figure 4). The polymorphic structure of

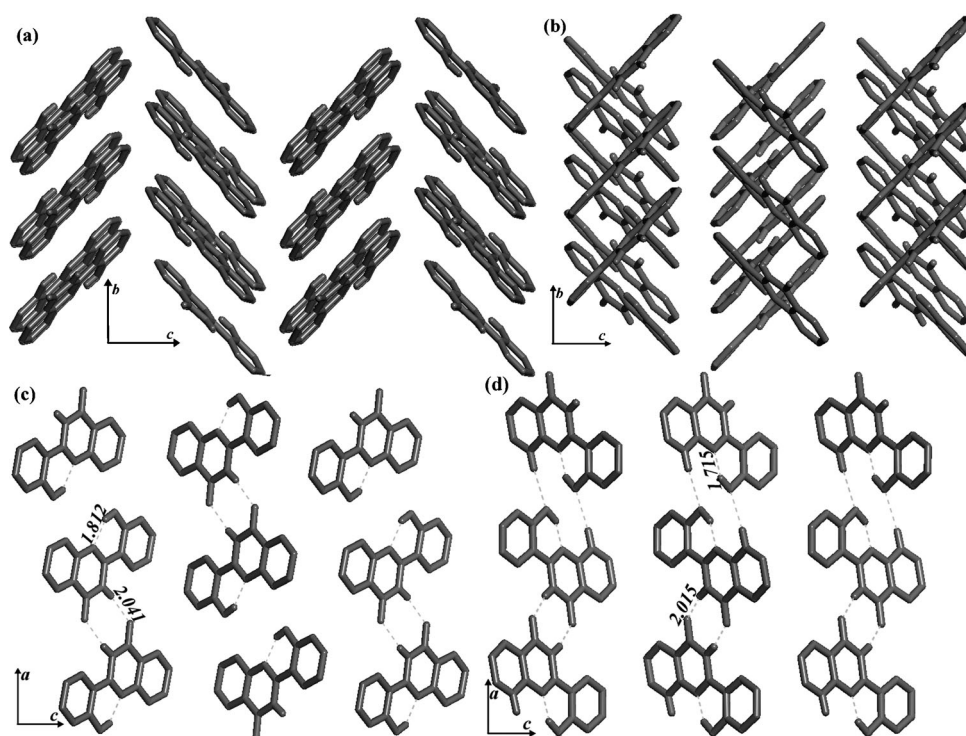


Figure 2. Molecular packing and selected H-bond interactions in the crystal lattice of a,c) HPQ-B and b,d) HPQ-BG. Only H atoms involved in H-bond interactions are shown. H-bonds are given as dashed lines. Corresponding distances (d_{HA} (A = H-bond acceptor), Å) are marked.

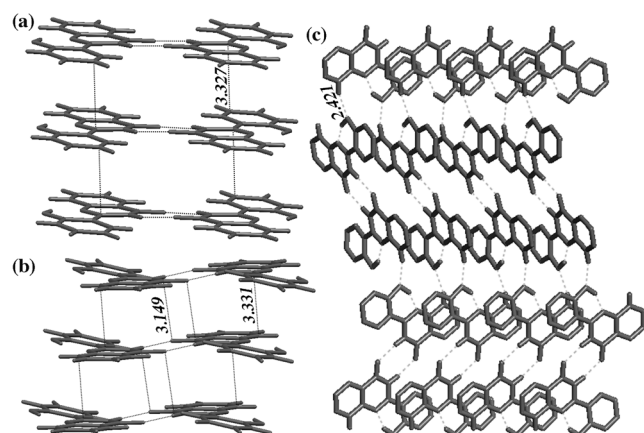


Figure 3. a) $\pi\cdots\pi$ interactions in HPQ-B and b,c) $\pi\cdots\pi$, C=O \cdots C=O dipolar and OH \cdots H-C interactions in HPQ-BG crystal lattices. In (c), only H atoms involved in H-bond interactions are shown. Weak interactions are given as broken lines; distances (Å) of H-bonds (d_{HA}) and other interaction are marked.

HPQ leads to the formation of tunable organic solid-state fluorescence materials. HPQ-B fluoresces at 497 nm while HPQ-BG fluoresces at 511 nm (Figure 5). The fluorescence intensity of HPQ-B and HPQ-BG were compared by keeping the optical density around 0.5 in KBr pellets of the respective sample. HPQ-B shows slightly higher fluorescence intensity than HPQ-BG (Figure S1 in the Supporting Information). In general, compounds with twisted conformations

exhibit fluorescence at shorter wavelengths than their non-twisted counterparts, since the latter can form closer molecular packing in the solid state that could facilitate excited energy transfer between molecules more easily.^[6] But in HPQ, more twisted HPQ-BG exhibits fluorescence at a longer wavelength than HPQ-B. This behavior is because more pronounced twisting of HPQ in HPQ-BG leads to stronger H-bonds and other intermolecular interactions, which result in closer packing of HPQ molecules in the crystal lattice (Figure 2 and Figure 3).

In spite of its good photo-physical properties^[10] and metal-chelating hydroxy pyridyl functional group that has the potential to display chelation-dependent fluorescence through coordination with metal ions, HPQ solution photophysics and

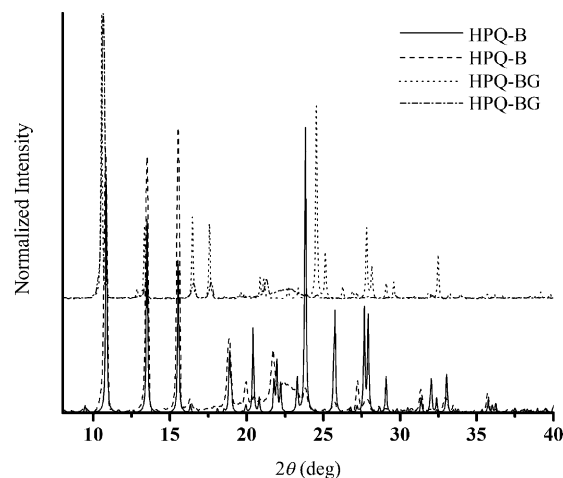


Figure 4. PXRD patterns of HPQ-B and HPQ-BG. Patterns represent calculations from single-crystal data ((—) and (.....)) and experimental data ((- - -) and (- · - ·)).

its chemical-sensor properties have never been explored in detail. HPQ shows weak to strong fluorescence in the visible region in dilute solution with different fluorescence λ_{max} due to solvatochromism. In ethyl acetate, HPQ showed weak fluorescence at $\lambda_{\text{max}}=507$ nm (quantum yield $\Phi=0.005$ on comparison with quinine sulfate), and in DMF it showed strong fluorescence λ_{max} at 457 nm ($\Phi=0.21$). It also showed similar fluorescence intensity in DMSO. The absorption

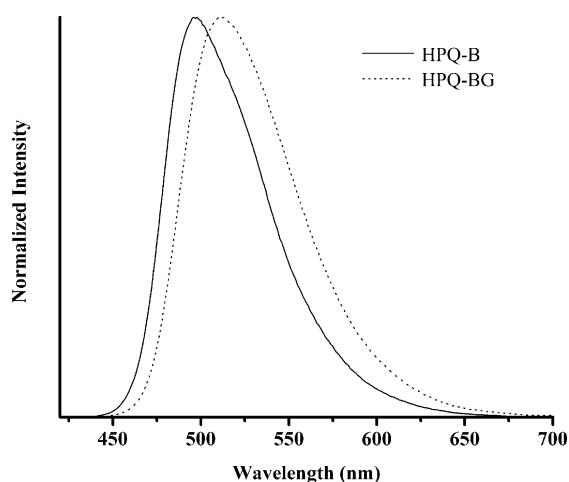


Figure 5. Normalized solid-state fluorescence of HPQ-B and HPQ-BG (excitation $\lambda_{\text{max}} = 370$ nm).

spectrum of free HPQ was examined using solvents of different polarity (Figure 6a). In DMF and DMSO, HPQ showed two absorption bands: an intramolecular charge-transfer band at 390–400 nm and an $n-\pi^*$ band at 335–339 nm. In other solvents (MeOH, acetone, and acetonitrile), the intramolecular charge-transfer band blue-shifted to 340–346 nm as small shoulder, and there was a clear $n-\pi^*$ absorption band at 331 nm. The addition of Zn^{2+} or Cd^{2+} metal ions to the HPQ DMF solution completely quench the intramolecular charge-transfer absorption band without altering the $n-\pi^*$ absorption band (Figure 6b).

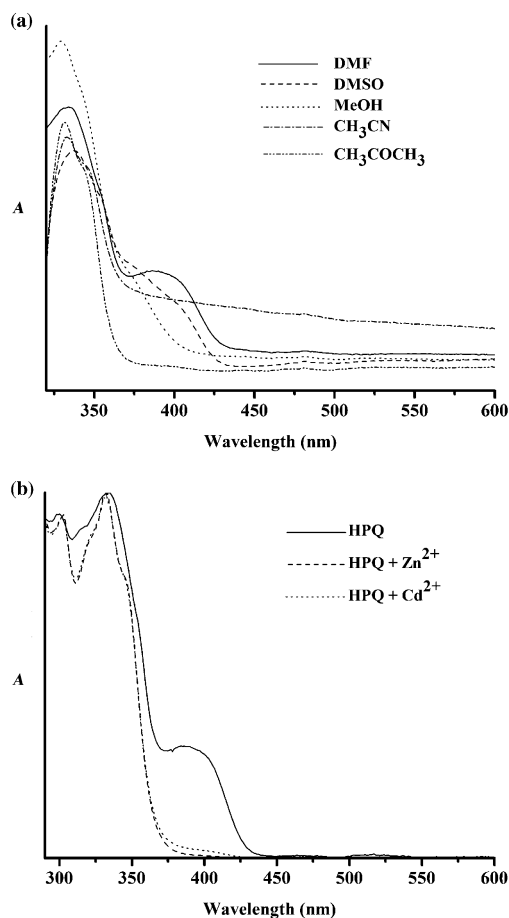


Figure 6. Absorbance spectra of HPQ a) in different solvents and b) with Zn^{2+} and Cd^{2+} metal ions in DMF.

trile), the intramolecular charge-transfer band blue-shifted to 340–346 nm as small shoulder, and there was a clear $n-\pi^*$ absorption band at 331 nm. The addition of Zn^{2+} or Cd^{2+} metal ions to the HPQ DMF solution completely quench the intramolecular charge-transfer absorption band without altering the $n-\pi^*$ absorption band (Figure 6b).

Interestingly, addition of Zn^{2+} and Cd^{2+} ions to HPQ not only blue-shifted the fluorescence λ_{max} of HPQ but also led to different λ_{max} for both metal ions. Addition of Zn^{2+} blue-shifts the λ_{max} from 497 to 420 nm, whereas Cd^{2+} addition blue-shifts HPQ fluorescence λ_{max} to 426 nm (Figure 7). The reason for the differences in λ_{max} is not clear, since single crystals of HPQ-Zn and HPQ-Cd could not be obtained to study the structural organization in the solid state. It is well known that the hydroxy pyridyl ligand generally forms 2:1 ligand/metal complexes.^[18] Fluorescence studies of HPQ with different concentrations of metal ions also indicate that HPQ might be forming a 2:1 HPQ- $\text{Zn}^{2+}/\text{Cd}^{2+}$ complex (Figure 7). Addition of 0.1 equivalents of Zn^{2+} to HPQ (10 μM) clearly changes the fluorescence spectrum profile,

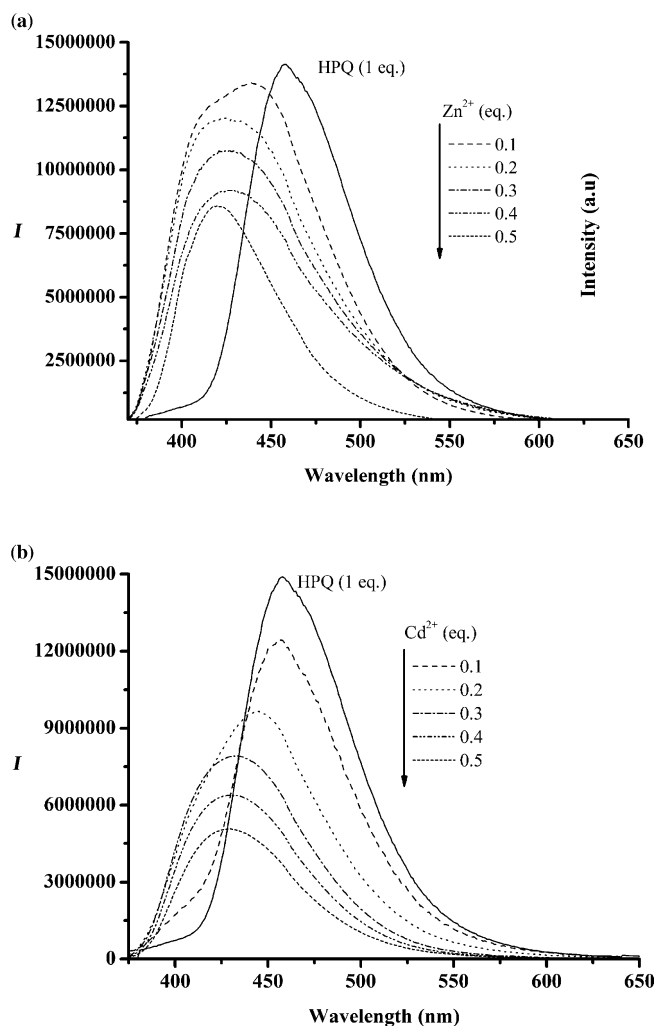


Figure 7. Fluorescence spectra of HPQ (10 μM) upon addition of a) Zn^{2+} and b) Cd^{2+} metal ions in DMF (excitation $\lambda_{\text{max}} = 345$ nm).

blue-shifting the λ_{\max} and reducing the intensity. Blue shift of λ_{\max} continued for addition of up to 0.5 equivalents Zn^{2+} and remained stable on further addition. Although the first addition of Cd^{2+} (0.1 equivalents) only reduced the fluorescence intensity, the subsequent additions led to blue shift of λ_{\max} with intensity reduction. Similar to Zn^{2+} , fluorescence λ_{\max} remained the same for addition of Cd^{2+} beyond 0.5 equivalents.

The selectivity of HPQ for Zn^{2+} and Cd^{2+} ions was confirmed by monitoring fluorescence spectrum with addition of other metal ions into the HPQ solution (Figure 8). Alka-

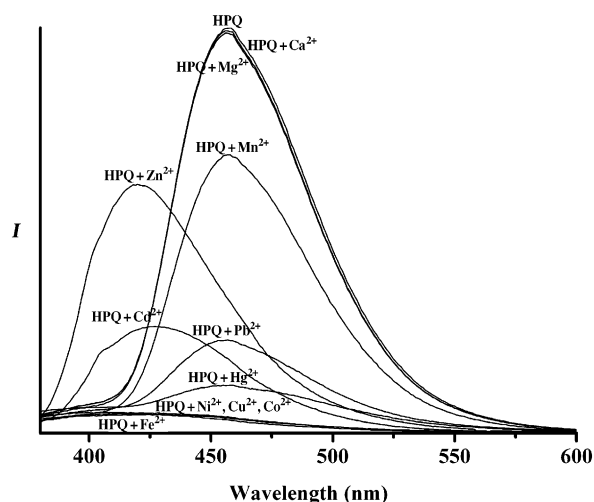


Figure 8. Fluorescence spectra of HPQ (10 μM) upon addition of metal salts (10.0 equivalents) in DMF (excitation $\lambda_{\max} = 345 \text{ nm}$).

line-earth-metal ions (Mg^{2+} and Ca^{2+}) did not have any influence on HPQ fluorescence. However, addition of transition and P-block metal ions (Mn^{2+} , Fe^{3+} , Hg^{2+} , and Pb^{2+}) have varied influence on the HPQ fluorescence. Fe^{3+} completely quenches the fluorescence, whereas Mn^{2+} , Pb^{2+} , and Hg^{2+} only reduced the fluorescence intensity without changing λ_{\max} . But Co^{2+} , Ni^{2+} , and Cu^{2+} reduced the fluorescence intensity as well as blue-shifting the λ_{\max} to 424 nm. No change in fluorescence wavelength and intensity was observed upon changing of the counteranion of the salt used to add Zn^{2+} and Cd^{2+} cation. Addition of Fe^{3+} into HPQ-Zn and HPQ-Cd solution completely quenches the fluorescence, and other transition-metal ions except Mn^{2+} reduce the fluorescence intensity of HPQ-Zn and HPQ-Cd solutions. This result indicates that those metal ions bind more strongly with HPQ than Zn^{2+} and Cd^{2+} .

Conclusions

Both tunable solid-state fluorescence as well as selective metal-ion-sensing properties was demonstrated in a single organic fluorescent material. Polymorphism of HPQ in THF leads to the tunable solid-state fluorescence. The larger con-

formational twist between phenyl and quinazolinone rings of HPQ molecules in HPQ-BG than HPQ-B leads to the formation of additional C-H...O intermolecular interactions and $\text{C}=\text{O}^{\delta-}\cdots\text{C}^{\delta+}=\text{O}$ dipolar interactions in the crystal lattice. Importantly, HPQ not only selectively senses Zn^{2+} and Cd^{2+} metal ions in DMF, but it also distinguishes between them. Tunable solid-state fluorescence and selective Zn^{2+} and Cd^{2+} metal-ion-sensing properties of HPQ makes it an interesting material for optoelectronic as well as biological sensor applications.

Experimental Section

Chemicals: 2-Hydroxybenzonitrile, 2-fluorobenzonitrile, anhydrous K_2CO_3 , dimethylsulfoxide (DMSO), NaOH, methanol, absolute ethanol, and metal salts were obtained from Aldrich and used as received. O,O'-CN was synthesized according to the literature procedure.^[19]

Synthesis of 2-(2-hydroxyphenyl)-4(3H)-quinazolinone (HPQ): O,O'-diphenyl cyano ether (0.5 g, 2.2 mmol) and sodium hydroxide (0.8 g, 20 mmol) was dissolved in 80 mL of water/ethanol mixture (60:40), and the reaction mixture was heated at reflux overnight. After the reaction mixture was cooled to room temperature, the solution was acidified using dilute hydrochloric acid. A white precipitate formed near pH 4. The precipitate was filtered, washed with distilled water, and dried under vacuum. Yield: 0.53 g (98%). Mp: 298 °C. NMR ($[\text{D}_6]\text{DMSO}$) ^1H : $\delta = 8.21\text{--}8.12$ (2H, m), 7.84–7.73 (2H, m), 7.54–7.47 (2H, m), 6.99–6.92 ppm (2H, m); ^{13}C : $\delta = 161.9, 160.5, 154.2, 146.5, 135.5, 134.7, 128.1, 127.4, 126.5, 121.1, 119.3, 118.3, 114.2$ ppm. MS: $m/z = 238$.

Crystallization of HPQ from ethyl acetate, acetone, DMF, DMSO, and methanol produced exclusively blue-green fluorescent crystals (HPQ-B), whereas crystallization from THF produced both blue and blue-green fluorescent crystals (HPQ-B and HPQ-BG).

Crystal data: HPQ-B (ccdc-809552): $\text{C}_{14}\text{H}_{10}\text{N}_2\text{O}_2$, $M = 238.24$, monoclinic, space group $P2_1/n$, $a = 13.378(3)$, $b = 5.136(10)$, $c = 16.648(3)$ Å, $\beta = 101.62(3)$, $V = 1120.6(4)$ Å³, $Z = 4$, $T = 150 \text{ K}$, 5844 reflections measured, 1947 unique ($R_{\text{int}} = 0.0224$), Final R values: 0.0388, wR : 0.1063; HPQ-BG (ccdc-809553): $\text{C}_{14}\text{H}_{10}\text{N}_2\text{O}_2$, $M = 238.24$, monoclinic, space group $C2/c$, $a = 30.496(6)$, $b = 4.984(1)$, $c = 16.804(3)$ Å, $\beta = 119.53(3)$, $V = 2222.3(10)$ Å³, $Z = 8$, $T = 123 \text{ K}$, 7867 reflections measured, 2764 unique ($R_{\text{int}} = 0.0241$), Final R values: 0.0496, wR : 0.1364.

Spectroscopic characterization: Absorption and fluorescence spectra were recorded using Perkin Elmer Lambda 1050 and Horiba Jobin Yvon Fluorolog instruments. Other metal-ion-selectivity measurements were performed by adding excess amounts of metal salt (10:1) to HPQ solution. Similarly, HPQ ligand binding with other metal ions compare to Zn^{2+} and Cd^{2+} were performed by adding excess metal salt (10:1) into HPQ-Zn/Cd solution. Solid-state fluorescence was measured by spreading the powdered samples on a glass plate. To compare the intensity of the solid-state fluorescence, transparent KBr pellets of HPQ-B and HPQ-BG were prepared, and the concentration of the compounds in solid matrix was adjusted to keep the optical density (OD) around 0.5. KBr pellets of these samples show similar fluorescence λ_{\max} as their pure solid samples.

Structural analysis: PXRD measurements were recorded using Siemens diffraktometer-D500 at room temperature. For single-crystal structure determinations, crystals were carefully chosen after they were viewed through a polarizing microscope. The crystals were glued to a thin glass fiber using an adhesive (cyano acrylate) and mounted on a diffractometer equipped with an APEX CCD area detector. The data collection was carried out at 150 K and no extraordinary methods were employed, except that the crystals were smeared in NIH immersion oil to protect them from ambient laboratory conditions. The intensity data were processed using Bruker's suite of data-processing programs (SAINT), and absorption corrections were applied using SADABS.^[20] The structure solution of all the complexes was carried out by direct methods, and refinements

were performed by full-matrix least-squares on F^2 using the SHELXTL-PLUS^[21] suite of programs. All the structures converged to good R factors. All the non-hydrogen atoms were refined anisotropically, and the hydrogen atoms were fixed on calculated position using appropriate HFIX options in SHELXTL and were refined isotropically. Intermolecular interactions were computed using the PLATON program.^[22]

Acknowledgements

The financial support from SASTRA University (TRR fund) is acknowledged with gratitude. The author is thankful to Dr. Sunil Varughese for his helpful discussions.

- [1] a) S. R. Forrest, *Nature* **2004**, 428, 911; b) Y. Taniguchi, *J. Photopolym. Sci. Technol.* **2002**, 15, 183; c) H. Kobayashi, M. Ogawa, R. Alford, P. L. Choyke, Y. Urano, *Chem. Rev.* **2010**, 110, 2620; d) L. Basabe-Desmonts, D. N. Reinhoudt, M. Crego-Calama, *Chem. Soc. Rev.* **2007**, 36, 993; e) C. J. Bhongale, C.-S. Hsu, *Angew. Chem.* **2006**, 118, 1432; *Angew. Chem. Int. Ed.* **2006**, 45, 1404; f) J. Feng, K. Tian, D. Hu, S. Wang, S. Li, Y. Zeng, Y. Li, G. Yang, *Angew. Chem.* **2011**, 123, 8222; *Angew. Chem. Int. Ed.* **2011**, 50, 8072; g) X. Luo, J. Li, C. Li, L. Heng, Y. Q. Dong, Z. Liu, Z. Bo, B. Z. Tang, *Adv. Mater.* **2011**, 23, 3261.
- [2] a) Y. Shirota, *J. Mater. Chem.* **2005**, 15, 75; b) H. Yersin, *Highly Efficient OLEDs with Phosphorescent Materials*, Wiley-VCH, Weinheim, **2008**; c) K. Müllen, U. Scherf, *Organic Light-Emitting Devices. Synthesis Properties and Applications*, Wiley-VCH, Weinheim, **2006**; d) E. Kim, S. B. Park, *Chem. Asian J.* **2009**, 4, 1646.
- [3] a) S. Mizukami, H. Houjou, K. Sugaya, E. Koyama, H. Tokuhisa, T. Sasaki, M. Kanesato, *Chem. Mater.* **2005**, 17, 50; b) Y. Ooyama, T. Okamoto, Y. Yamaguchi, T. Suzuki, A. Hayashi, K. Yoshida, *Chem. Eur. J.* **2006**, 12, 7827; c) Z. Fei, N. Kocher, C. J. Mohrschladt, H. Ihmels, D. Stalke, *Angew. Chem.* **2003**, 115, 807; *Angew. Chem. Int. Ed.* **2003**, 42, 783; d) Y. Ooyama, K. Yoshida, *New J. Chem.* **2005**, 29, 1204.
- [4] a) R. Davis, N. P. Rath, S. Das, *Chem. Commun.* **2004**, 74; b) T. Mutai, H. Satou, K. Araki, *Nat. Mater.* **2005**, 4, 685; c) H. Zhang, Z. Zhang, K. Ye, K. Zhang, Y. Wang, *Adv. Mater.* **2006**, 18, 2369; d) C. Kitamura, T. Ohara, N. Kawatsuki, A. Yoneda, T. Kobayashi, H. Naito, T. Komatsu, T. Kitamura, *CrystEngComm* **2007**, 9, 644; e) Y. Fan, Y. Zhao, L. Ye, B. Li, G. Yang, Y. Wang, *Cryst. Growth Des.* **2009**, 9, 1421; f) S. P. Anthony, S. M. Draper, *J. Phys. Chem. C* **2010**, 114, 11708.
- [5] a) A. M. Talarico, I. Aiello, A. Bellusci, A. Crispini, M. Ghedini, N. Godbert, T. Pugliese, E. Szerb, *Dalton Trans.* **2010**, 39, 1709; b) J. S. Field, L. P. Ledwaba, O. Q. Munro, D. R. McMillin, *CrystEngComm* **2008**, 10, 740; c) W. W. W. Yam, K. M. C. Wong, N. Zhu, *J. Am. Chem. Soc.* **2002**, 124, 6506; d) M. Brinkmann, G. Gadret, M. Muccini, C. Taliani, N. Masciocchi, A. Sironi, *J. Am. Chem. Soc.* **2000**, 122, 5147.
- [6] T. Mutai, H. Tomoda, T. Ohkawa, Y. Yabe, K. Araki, *Angew. Chem.* **2008**, 120, 9664; *Angew. Chem. Int. Ed.* **2008**, 47, 9522.
- [7] a) Q. Liu, M. S. Mudadu, R. Thummel, Y. Tao, S. Wang, *Adv. Funct. Mater.* **2005**, 15, 143; b) A. Wakamiya, K. Mori, S. Yamoguchi, *Angew. Chem.* **2007**, 119, 4351; *Angew. Chem. Int. Ed.* **2007**, 46, 4273.
- [8] a) Y. Mizobe, M. Miyata, I. Hisaki, Y. Hasegawa, N. Tohnai, *Org. Lett.* **2006**, 8, 4295; b) Y. Mizobe, N. Tohnai, M. Miyata, Y. Hasegawa, *Chem. Commun.* **2005**, 1839; c) Y. Mizobe, T. Hinoue, A. Yamamoto, I. Hisaki, M. Miyata, Y. Hasegawa, N. Tohnai, *Chem. Eur. J.* **2009**, 15, 8175; d) S. P. Anthony, S. Varughese, S. M. Draper, *Chem. Commun.* **2009**, 7500; e) S. P. Anthony, S. Varughese, S. M. Draper, *J. Phys. Org. Chem.* **2010**, 23, 1074.
- [9] a) P. Jiang, Z. Guo, *Coord. Chem. Rev.* **2004**, 248, 205; b) R. B. Thompson, *Curr. Opin. Chem. Biol.* **2005**, 9, 526; c) S. Sreejith, K. P. Divya, A. Ajayaghosh, *Chem. Commun.* **2008**, 2903; d) W. Liu, L. Xu, R. Sheng, P. Wang, H. Li, S. Wu, *Org. Lett.* **2007**, 9, 3829; e) N. C. Lim, H. C. Freake, C. Brückner, *Chem. Eur. J.* **2005**, 11, 38.
- [10] a) J. M. Berg, Y. Shi, *Science* **1996**, 271, 1081; b) X. Xie, T. G. Smart, *Nature* **1991**, 349, 521; c) E. M. Nolan, S. J. Lippard, *Acc. Chem. Res.* **2009**, 42, 193.
- [11] a) T. Jin, J. Lu, M. Nordberg, *Neurotoxicology* **1998**, 19, 529; b) S. Satarug, J. R. Baker, S. Urbenjapol, M. Haswell-Elkins, P. E. B. Reilly, D. J. Williams, M. R. Moore, *Toxicol. Lett.* **2003**, 137, 65.
- [12] a) K. Komatsu, K. Kikuchi, H. Kojima, Y. Urano, T. Nagano, *J. Am. Chem. Soc.* **2005**, 127, 10197; b) L. Zhang, R. J. Clark, L. Zhu, *Chem. Eur. J.* **2008**, 14, 2894; c) E. M. Nolan, J. W. Ryu, J. Jaworski, R. P. Feazell, M. Sheng, S. J. Lippard, *J. Am. Chem. Soc.* **2006**, 128, 15517; d) K. Komatsu, K. Kikuchi, H. Kojima, Y. Urano, T. Nagano, *J. Am. Chem. Soc.* **2004**, 126, 12470; e) L. Xue, Q. Liu, H. Jiang, *Org. Lett.* **2009**, 11, 3454.
- [13] a) D. L. Williams, A. Heller, *J. Phys. Chem.* **1970**, 74, 4473; b) A. U. Khan, M. Kasha, *Proc. Natl. Acad. Sci. USA* **1983**, 80, 1767; c) J. J. Naleway, C. M. J. Fox, D. Robinhold, E. Terpetschnig, N. A. Olson, R. P. Haugland, *Tetrahedron Lett.* **1994**, 35, 8569; d) Z. Diwu, Y. Lu, R. H. Upson, M. Zhou, D. H. Klaubert, R. P. Haugland, *Tetrahedron* **1997**, 53, 7159.
- [14] X. B. Zhang, G. Chenga, W.-J. Zhang, G. L. Shen, R.-Q. Yu, *Talanta* **2007**, 71, 171.
- [15] a) R. Pater, *J. Heterocycl. Chem.* **1971**, 8, 699; b) J. Petridou-Fischer, E. P. Papadopoulos, *J. Heterocycl. Chem.* **1983**, 20, 1159; c) A. A. Layeva, E. V. Nosova, G. N. Lipunova, T. V. Trashakhova, V. N. Charushinb, *Russ. Chem. Bull. Int. Ed.* **2007**, 56, 1821; d) M. Kidwai, Priya, *Indian J. Chem. Soc.* **2007**, 47B, 1876; e) M. Bakavoli, A. Shiri, Z. Ebrahimpour, M. Rahimizadeh, *Chin. Chem. Lett.* **2008**, 19, 1403.
- [16] a) S. P. Anthony, K. Basavaiah, T. P. Radhakrishnan, *Cryst. Growth Des.* **2005**, 5, 1663; b) G. R. Desiraju, *Acc. Chem. Res.* **1996**, 29, 441.
- [17] a) S. Lee, A. B. Mallik, D. C. Fredrickson, *Cryst. Growth Des.* **2004**, 4, 279; b) H. B. Buerger, J. D. Dunitz, *Acc. Chem. Res.* **1983**, 16, 153.
- [18] P. A. Vigato, S. Tamburini, *Coord. Chem. Rev.* **2008**, 252, 1871.
- [19] F. Li, Q. Wang, Z. Ding, F. Tao, *Org. Lett.* **2003**, 5, 2169.
- [20] G. M. Sheldrick, SADABS, *Area Detector Correction*. 2002. Madison, WI, Siemens Industrial Automation, Inc.
- [21] a) G. M. Sheldrick, SAINT *Area Detector Integration Software*. **1998**. Madison, WI, Siemens Industrial Automation, Inc; b) G. M. Sheldrick, SHELX97 Programs for Crystal Structure Analysis. (97–2). 1998. Institut für Anorganische Chemie der Universität; c) G. M. Sheldrick, XPRED. (V5.1). **1997**. Madison, WI, Bruker Analytical X-Ray Systems.
- [22] PLATON. A. L. Spek, *Acta Crystallogr. Sect. A* **1990**, 46, C34.

Received: October 6, 2011

Published online: December 19, 2011